

1 **Sub-synoptic-scale features associated with extreme surface gusts in UK extra-tropical**
2 **cyclone events**

3 **N Earl^{1,2}, S. Dorling¹, M. Starks¹ and R. Finch¹**

4 ¹ School of Environmental Sciences, University of East Anglia, Norwich Research Park,
5 Norwich, Norfolk, NR4-7TJ, UK.

6 ² School of Earth Sciences, The University of Melbourne, Parkville, Melbourne, Victoria,
7 3010.

8 Corresponding Author: Nick Earl, nearl@unimelb.edu.au, +61390353848.

9

10 **Key points**

11

12 A novel way to quantify the relative contributions of mesoscale extra-tropical cyclone
13 features is introduced.

14

15 Larger scale features are most commonly associated with the top 1% of UK surface gusts but
16 smaller scale features generate the most extreme 0.1% of winds.

17

18 Sting jets and convective lines account for two-thirds of severe surface gusts in the UK.

19 **Abstract**

20 Numerous studies have addressed the mesoscale features within extra tropical cyclones
21 (ETCs) that are responsible for the most destructive winds, though few have utilised surface
22 observation data, and most are based on case studies. By using a 39-station UK surface
23 observation network, coupled with in-depth analysis of the causes of extreme gusts during the
24 period 2008-2014, we show that larger scale features (warm and cold conveyor belts) are
25 most commonly associated with the top 1% of UK gusts but smaller scale features generate
26 the most extreme winds. The cold conveyor belt is far more destructive when joining the
27 momentum of the ETC, rather than earlier in its trajectory, ahead of the approaching warm
28 front. Sting jets and convective lines account for two-thirds of severe surface gusts in the UK.

29

30 **Index terms and keywords**

31

32 3309 Climatology

33 3329 Mesoscale meteorology

34 4307 Methods

35 4313 Extreme events

36

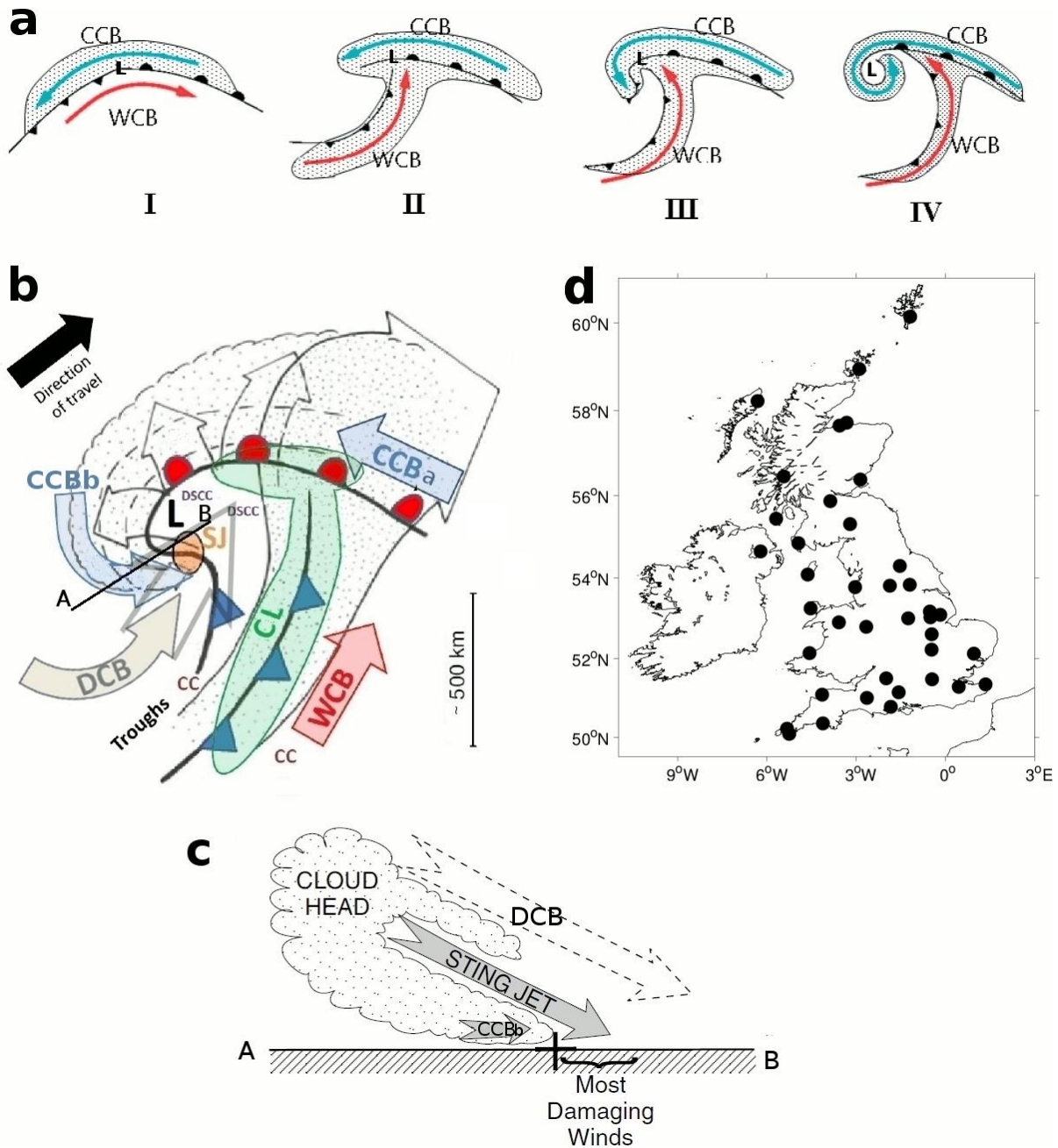
37 Extra tropical cyclones, extreme surface winds, surface observations, mesoscale features,
38 sting jets, convective lines

39 1. Introduction

40 European extra tropical cyclones (ETCs) are the most economically significant weather
41 hazard when averaging insured losses over multiple years, as exemplified by the ‘16th
42 October 1987 Storm’ in the UK [Woodroffe, 1988; Browning, 2004], by Windstorm Gudrun
43 of 2005 [Baker, 2009] and by Windstorm Kyrill of 2007 [Brönnimann *et al.*, 2012]. From
44 1970-2015, 32 of the 40 most expensive world-wide insured loss events were weather related,
45 nine of which were located in Europe and associated with ETCs, generating hurricane force
46 surface winds and widespread flooding [Swiss Re, 2016]. This paper explores the mesoscale
47 features within ETCs which are associated with observed extreme surface winds.

48

49 There has been much research addressing the synoptic scale structure of ETCs since the
50 development of the Norwegian cyclogenesis model [Bjerknes and Solberg, 1922]. It was the
51 first conceptualised ETC life-cycle model, locating cyclogenesis along the polar front and
52 dividing the cycle into stages of the typical life of a low pressure system in the extra-tropics
53 [Parton *et al.*, 2010]. Development of the ETC life-cycle conceptual model evolved into the
54 conveyor belt paradigm [Browning, 1990; figure 1b] and the development of the *Shapiro and*
55 *Keyser* [1990] cyclone model (figure 1a). In addition, *Schultz and Vaughan* [2011] provided a
56 modified view of the occlusion front paradigm within the Norwegian cyclogenesis model
57 suggesting that viewing the occlusion process as wrap-up rather than catch-up resolves
58 anomalies within the conceptual model.



59

60 **Figure 1. a.** Shapiro-Keyser conceptual model of the life cycle of an extra-tropical cyclone:
 61 (I) open wave, (II) frontal fracture, (III) bent-back front and frontal T-bone, and (IV) mature,
 62 frontal seclusion. The cold and warm conveyor belts (CCB and WCB respectively) are
 63 marked along with the low pressure centre (L) and the cloud signature (stippled areas)
 64 [adapted from *Baker, 2009*]. **b.** Conceptual model of sub-synoptic-scale features within an
 65 extra-tropical cyclone, during transition from stage III to stage IV (adapted from *Browning,*
 66 *2004*). See tables 1 and S1 for an explanation of WCB, CCBa, CCBb, DCB, SJ (orange
 67 shading), CC, CL (green shading) and DSCC. **c.** Vertical cross-section through the A-B line
 68 (in b), displaying the relative positions of the conveyor-belts seen during sting jets and the
 69 region of cloud [adapted from *Clark et al., 2005*]. **d.** Locations of the 39 UK wind monitoring
 70 sites used in this study.

71

72 *Browning* [2004] identified one of the causes of the most extreme surface winds to be
73 associated with a mesoscale feature at the tip of the cloud head as the ‘sting at the end of the
74 tail’ (shortened to sting jet; SJ) (table 1; figure 1b). This proved to be the case for the ‘16th
75 October 1987 Storm’ [*Clark et al.*, 2005], for Windstorm Jeanette in October 2002 [*Parton et*
76 *al.*, 2009] and Christian in October 2013 [*Browning et al.*, 2015] amongst others. However
77 *Baker* [2009] found that the strongest surface winds during Windstorm Gudrun of January
78 2005 were associated with the cold conveyor belt (CCB) as it wrapped around the low
79 pressure centre and acted in the same direction as the motion of the cyclone. *Hewson and Neu*
80 [2015] broke down storms into distinct features, SJ, CCB and warm-conveyor belt (WCB)
81 explaining where the extreme surface winds occur in relation to a typical ETC track. The
82 WCB starts at low levels before rising over the warm front above the cold air below. It is
83 most likely to affect the surface in the warm sector, just ahead of the cold front, rather than
84 nearer the warm front where it has been forced upwards (figure 1b). The WCB produces the
85 largest footprint of strong surface winds, though these are not as severe as the CCB or SJ
86 [*Hewson and Neu*, 2015]. *Clark* [2013] developed a climatology of convective lines (CL;
87 comprising mainly narrow cold frontal rain-bands (NCFR) and post-frontal quasi-linear
88 convective systems (QLCSs)). These lines of organised and strong convection occur mainly
89 along cold frontal boundaries in the UK, though a few occur in association with occluded
90 fronts. Pre-frontal QLCSs were not included in *Clark’s* [2013] climatology. This CL
91 climatology was not constructed with surface wind gusts in mind; however CLs, especially
92 QLCSs, are well-known for producing strong winds, including intense downburst winds, a
93 rear inflow jet [*Weisman*, 2001] and low-level mesovortices, all of which produce damaging
94 winds [*Davis et al.*, 2004; *Wheatley et al.*, 2006]. The rear inflow jet and mesovortices
95 usually travel perpendicular to the orientation of the line, as distinct from the winds within
96 the parallel-flowing WCB, which is found ahead of many narrow cold frontal rain bands in
97 ETCs [*Browning*, 2004]. QLCSs are particularly common in the USA and are sometimes
98 known as squall lines. QLCSs that present a strongly-bulging structure are referred to as bow
99 echoes [*Weisman*, 2001]. These systems have also been reported in Europe [*Gatzen et al.*,
100 2011].

101

102 Table 1 summarises the characteristics of the conveyor belts and other ETC sub-synoptic-
103 scale features and Figure 1b displays the respective locations of these features within a

104 Shapiro-Keyser conceptual ETC, where the highest surface impacts are likely during
105 transition from stage III to stage IV of the Shapiro-Keyser conceptual model of the life cycle.
106 The A-B cross section in figure 1c shows the relative vertical positions of the SJ, CCBb and
107 the dry conveyor belt (DCB) in ETCs which possess a well-developed SJ that reaches the
108 surface.

109

110 Not all ETCs will follow the Shapiro-Keyser conceptual model life cycle, depending on
111 whether the ETC is embedded in diffluent or confluent large-scale flow in the upper-levels
112 and, if the former, will tend to follow a life-cycle more akin to the Norwegian life-cycle
113 model as explored by *Schultz et al.* [1998]. Also, many ETCs will not contain all of these
114 sub-synoptic-scale features, some for example exhibit insufficient deepening rate (< 1
115 Bergeron), a major factor in producing SJs [*Browning, 2004*]. Furthermore, sub-synoptic-
116 scale features may be present in many ETCs, such as a SJ or DCB, but their presence may not
117 result in an extreme gust being recorded at the surface. However all features shown in figure
118 1b have been observed to cause extreme surface windspeeds in some ETCs.

119

120 Most studies rely on tracking algorithms for intense ETC identification, often based on re-
121 analysis resolution data [*Neu et al., 2013, Hewson and Neu, 2015*]. Many mesoscale features
122 are sub-grid scale for these, so the intensity of surface winds is poorly represented. This paper
123 introduces a novel way to quantify the relative contributions of mesoscale ETC features,
124 based on surface wind observations. The approach used here is distinct from previous
125 climatological studies, for example *Parton et al.* [2010], *Clark* [2013], and *Martínez-*
126 *Alvarado et al.* [2012], who used mid-tropospheric observations, radar imagery and ERA-
127 Interim data respectively, without specific reference to observed windspeeds at the surface. It
128 is also complementary to *Hewson and Neu* [2015] in their IMILAST project
129 ('Intercomparison of MId-LATitude STorm diagnostics', first described in *Neu et al., 2013*),
130 based on storm track algorithms

131 **2. Data and methods**

132 **2.1 Observational network and extreme wind identification**

133 The events used in this study are identified using the UK observational daily maximum gust
134 speed (DMGS) database, introduced by *Hewston and Dorling* [2011] and also analysed in
135 *Earl et al.* [2013]. This covers the period 1980-2014, consisting of 39 UK wind monitoring
136 sites (figure 1d). This research was completed in conjunction with an associated forecast
137 verification study [*Earl*, 2013], the data for which began in 2008, therefore the work
138 presented here covers the period 2008-2014. The DMGSs are ranked in order of intensity for
139 each of the 39 observational network sites and the top 1% (128 strongest DMGSs plus those
140 tied for rank 128) and 0.1% (13 strongest DMGSs; hereafter, 1%DMGS and 0.1%DMGS)
141 during the whole 1980-2014 period are highlighted at each site (placing the 2008-2014 period
142 into a longer context). The absolute wind speeds vary greatly throughout the network, with
143 the 99.9th percentile at Lerwick for example being 81kt, whereas at Heathrow, this percentile
144 was reached with just 55kt. During the development of a windstorm loss model, *Hewston*
145 [2008] found that it was only the top 2% of local DMGSs that resulted in damage to insured
146 property. Concentrating here on the 1%DMGSs and 0.1%DMGSs therefore places specific
147 emphasis on the most damaging winds. Each 1%DMGS and 0.1%DMGS is then associated
148 with a corresponding ETC (no other causes were evident during the period 2008-2014). ETC
149 names, as allocated by the Free University of Berlin, are used for the identified ETCs. Only
150 ETC events which are associated with more than one 1%DMGS, be it at more than one
151 station or a single station on successive days, are included in the study, to minimise the
152 possible impact of erroneous measurement data.

153 **2.2 Feature allocation**

154 Allocation of each of the 1%DMGS (or 0.1%DMGS) to associated sub-synoptic-scale
155 features (figure 1b) is undertaken manually, using surface pressure charts (courtesy of UK
156 Met Office), 15-minute rainfall radar images (from the UK Met Office NIMROD system) and
157 satellite imagery (courtesy of the University of Dundee Satellite Receiving Station), along
158 with the data from the surface observation network (accurate to 1 minute). Once the DMGS
159 has been identified, the most temporally applicable 6-hourly surface pressure charts are used
160 along with the applicable satellite images to identify the main features of the ETC and
161 establish the stage of Shapiro-Keyser life-cycle. These are then compared with the radar
162 images which are closest in time to the gust event for feature assignment (e.g. fronts, troughs
163 and low pressure centre). The high temporal resolution radar images are essential, providing
164 the opportunity to accurately track the cyclone features through time, highlighted by the

165 precipitation signature, until the time of the DMGS in question at the specific station. Table 1
 166 provides a description of the mechanism allocation. When a 1% (0.1%) DMGS is not judged
 167 to be associated with any sub-synoptic-scale feature, it is identified as being ‘unclassifiable’.
 168 Once all of the sub-synoptic-scale feature causes for all 1% (0.1%) DMGS have been
 169 categorised, they are then assembled as a 2008-2014 climatology of 1% (0.1%) DMGS gust-
 170 causing features. (See Figure S1 and Text S1 for three examples of 0.1% DMGS allocation).

171

172 **Table 1.** Allocations of features^a

| Feature | Description |
|---------------------------|---|
| Cold conveyor belt (CCBa) | DMGS occurs ahead (usually east) of the surface warm front, identified by the foregoing precipitation and cloud signatures in the satellite and radar images. The gust is often orientated parallel to the front travelling towards the low pressure centre. |
| Cold conveyor belt (CCBb) | DMGS is located equatorward or west of the low pressure centre, usually directly beneath (but not at the tip of) the cloud and precipitation signature. Pressure charts indicate high pressure gradients in this part of the ETC. The gust is usually orientated equatorward or in the direction of ETC travel, occurring in stage IV of the Shapiro-Keyser life cycle model. |
| Warm conveyor belt (WCB) | This usually broad region of poleward flowing air often affects the surface relatively early in the life cycle (stages II-III). Located between, but clearly separate from, the two primary fronts and often flows parallel to the cold front (rather than perpendicular as for CLs). |
| Dry conveyor belt (DCB) | The dry slot is in a region of clearing skies behind the cold front, clearly distinct from the main precipitation and cloud signatures in the radar and satellite images, with no radar echo or visible cloud. DMGS occurs in this region, with no sign of cellular convection apparent. |
| Convective Lines (CL) | Lines of organised and strong convection, very clear signal in the radar images. DMGS is usually travelling perpendicular to the orientation of the front line (distinct from the WCB). To be classified as a CL, the feature has to meet <i>Clark's</i> [2013] threshold criteria (see table S1) |
| Sting Jet (SJ) | DMGS at the tip of the cloud head hook often clearly visible in the radar and satellite images. Only identified in stages II and III of the Shapiro-Keyser life cycle model and replaced by the CCBb in stage IV. ETC must be rapidly deepening (\geq one Bergeron), there must be clear evidence of cloud banding and DMGS located within 100km of the cloud hook tip. |
| Dry Slot Cellular | Cellular convection that occurs within the dry slot producing heavy showers visible on the radar images at the site location during the time of |

| | |
|-------------------------------------|---|
| Convection (DSCC) | DMGS. |
| Cellular Convection (CC) | Area of unorganised convection outside of the dry intrusion producing heavy showers visible on the radar images at the site location during the time of DMGS. |
| Pseudo-Convective Lines (pseudo-CL) | As with CLs but do not reach the status of CL as defined by <i>Clark</i> [2013], though do possess the same distinct characteristics. Also included are lines visible on the radar images, which were classified as CLs earlier or later in the day but which were not so classified at the time of DMGS. |

173 ^a Description of allocating DMGSs to specific ETC features.

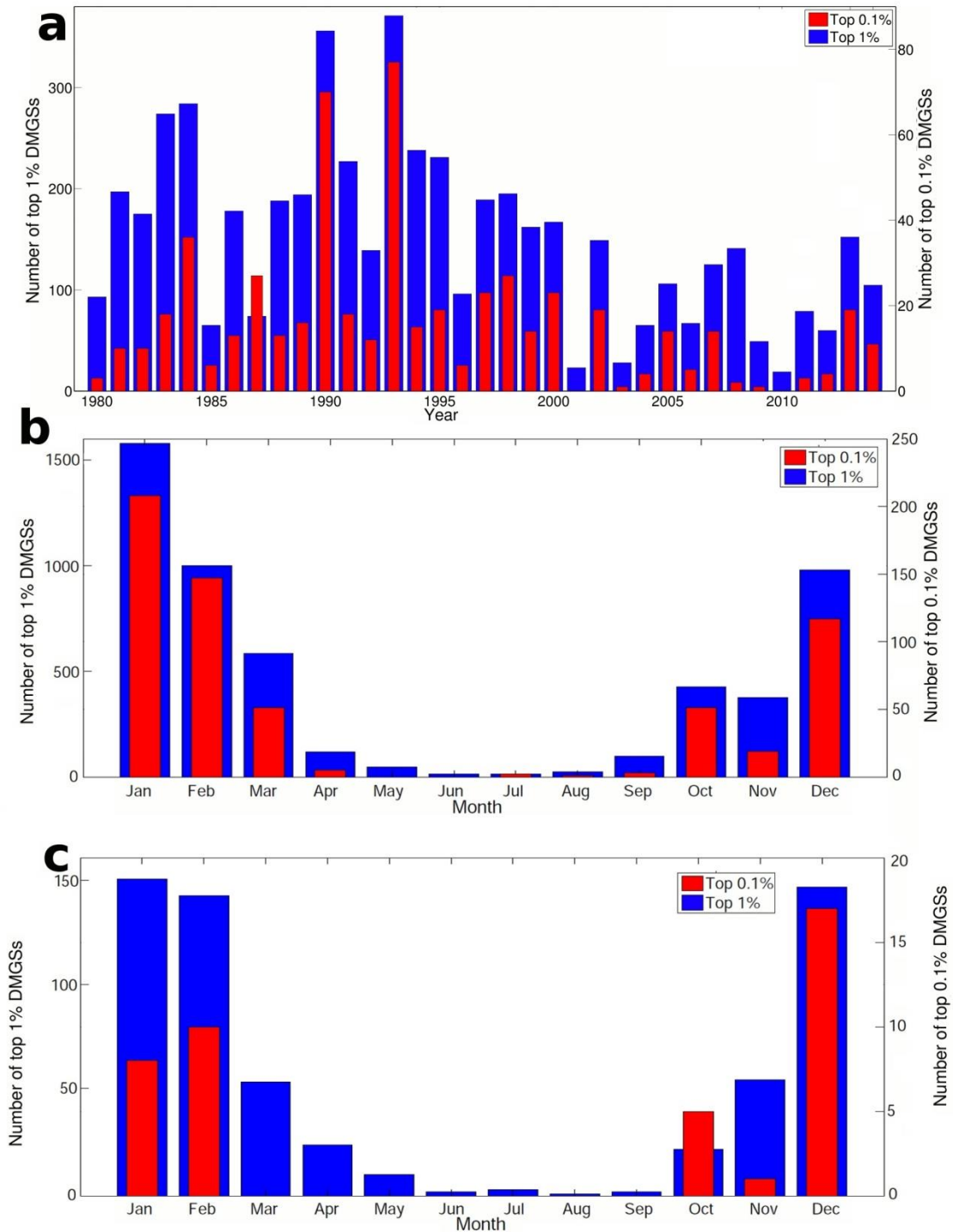
174

175 We acknowledge that some extreme gusts may be missed by our method due to the spatially
 176 irregular nature of the observation network (figure 1d), especially the smaller scale features
 177 such as SJs. Also, only including the DMGS (one per day per station) means omitting some
 178 extreme gusts seen on the same day often from a different mechanism.

179 3. Results

180 3.1 Inter- and intra-annual variability of 1980-2014 extreme DMGS

181 Results presented in *Earl et al.* [2013] showed that the years 2008-2010 saw a well-below-
 182 average frequency of high daily mean windspeeds compared to the early 1980s and early
 183 1990s. Since then there has been a recovery. Therefore, before analysing the 2008-2014
 184 1%DMGS and 0.1%DMGS observations, we explore the full 1980-2014 DMGS surface
 185 station measurement database to highlight the 2008-2014 period's relative contribution to
 186 1980-2014 extremes. This sets the 2008-2014 period in the context of the longer
 187 climatological record.



188

189 **Figure 2. a.** 1980-2014 inter-annual variability in the frequency of Top 1% (1%DMGS) and
 190 0.1% (0.1%DMGS) occurrences (totals : 5256 and 554 respectively) for all 39 stations. **b.**
 191 1980-2014 monthly distribution of 1%DMGSs and 0.1%DMGSs. **c.** 2008-2014 monthly
 192 distribution of 1%DMGSs and 0.1%DMGSs. Note – top 0.1% DMGS total is more than 507
 193 (39 sites x 13 (top 0.1% of 35 years)) due to DMGSs tied for rank 13 at some sites (same
 194 occurs with top 1%).

195

196 Figure 2a presents the 1980-2014 inter-annual distribution of 1%DMGS and 0.1%DMGS
197 totals, providing an insight into the main periods of extreme storminess. There is a large
198 inter-annual range for both percentiles, lowest in 2010 with just 19 occurrences of 1%DMGS
199 (0.4% of the 35-year total) and no 0.1%DMGS. Similarly low values occurred in 2001 and
200 2003. The highest values for both percentiles occurred during 1993 with 371 (7.1%) of
201 1%DMGSs and 77 (14%) of 0.1%DMGSs. The early 1980s and early 1990s stand out as
202 periods of more frequent extreme windspeeds, the 2000s much less so, in accordance with
203 other related mean wind speed studies in the literature for the UK and Europe as a whole
204 [Wang *et al.*, 2009; Vautard *et al.*, 2010; Earl *et al.*, 2013]. This is strongly linked to the
205 phase of the North Atlantic Oscillation [NAO; Earl *et al.*, 2013] and ETC activity in the
206 Atlantic [Tilinina *et al.*, 2013]. A positive NAO means a stronger pressure gradient between
207 the Icelandic low and Azores high, bringing more zonal conditions to the North Atlantic and
208 subsequently more windstorms to northern Europe. Since 2011, extreme windspeeds have
209 increased towards longer term average frequencies, but are still below average, in agreement
210 with recent NAO variability [Hanna *et al.*, 2015].

211

212 Generally 2008-2014 was a low-windspeed period; only 2013 recorded close to average
213 (~150) top 1%DMGS frequency. The 0.1%DMGSs show even “leaner” storminess in this
214 period, with an average of 8.2 occurrences per year, well below the annual average of 15.7
215 over the longer period. The unprecedented storminess of the early 1990s [Wang *et al.*, 2009;
216 Earl *et al.*, 2013], highlighted by the strongest positive NAO index on record [1899-2014;
217 Hanna *et al.*, 2014], can be seen to be largely due to exceptionally-stormy years in 1990 and
218 1993, neighbouring years being much closer to the 0.1%DMGS 35-year average. The years
219 2008 and 2013 accounted for twice the number of 1%DMGSs compared with the famous
220 1987, whereas the 1987 0.1%DMGSs outweigh those attributed to 2008 and 2013; there was
221 no 2008-2014 storm of a comparable magnitude to the ‘16th October 1987 Storm’ which, at
222 the time, set records for insured losses for a natural catastrophe [Swiss Re, 2016].

223

224 Figure 2b shows that winter months (DJF) in the 1980-2014 period account for 67.7% of
225 1%DMGS and 75.6% of 0.1%DMGS, January being the dominant contributor to both
226 percentiles followed by February and then December; winter is the time of year when

227 synoptic conditions best accommodate extreme ETCs to track across the UK due to the
228 higher pressure gradients across the region [Wang *et al.*, 2009]. The month of October, so
229 influential in 1987, is less prominent, though does account for more DMGS extremes than
230 November for both percentiles. The months from April to September rarely contribute to the
231 highest DMGSs. January experienced 208 (37.5%) of the total 0.1%DMGSs, January 1993
232 the stormiest of all, accounting for 58, including the mid-January Braer Storm producing 23
233 0.1%DMGSs. On January 25th 1990, Windstorm Daria produced 22 0.1%DMGSs on a single
234 day. Other prominent UK windstorms causing heavy insured losses and impacting the
235 0.1%DMGS climatology include Jeanette of late October 2002 (12 0.1%DMGS occurrences),
236 Erwin in January 2005 (12), Windstorm Kyrill on 18th January 2007 (14) and Xaver on 5th
237 December 2013 (7) (table S2). With high-profile storms featuring so prominently in the
238 extreme DMGS part of the observation database, additional confidence can be placed in its
239 ability to accurately represent the UK's extreme wind regime.

240

241 Figure 2c shows that the 2008-2014 monthly distribution of the 1%DMGSs is also dominated
242 by January, February and December. This period also continues the longer-term pattern of
243 more 0.1%DMGSs during October than November, indicating that this 7-year period
244 provides a good representation of the longer term record, despite being a period of “leaner”
245 storminess. With the relatively high number of October 0.1%DMGSs, along with no events
246 between March-September, the impact of October events will be enhanced due to summer
247 vegetation growth and trees often still being in leaf, a reason why the ‘16th October 1987
248 Storm’ was so damaging [Woodroffe, 1988; Browning, 2004]. The reason behind this October
249 spike is unclear, however, the analysis of ‘singularities’ in the post-World War II era, chiefly
250 by Lamb (1950), suggested that mid-November in the UK often includes an 11-day period of
251 calm anticyclonic weather. Lamb analysed the 1898-1947 temporal period, so there is no
252 overlap with our study, and the singularities theory is controversial, however this may
253 provide a possible explanation for the relative lull in November extreme wind activity.

254 **3.2. 2008-2014 storm set identification**

255 Despite the relatively low windiness of the 2008-2014 period, there were 600 examples of
256 1%DMGSs and 41 0.1%DMGSs experienced at the 39 network sites, from which a number

257 of individual windstorms may be identified. A total of 73 unique ETC events, shown in Table
 258 S2, each resulted in at least two occurrences of 1%DMGS.

259

260 Despite the lower overall frequency of strong wind events in this period, compared to the
 261 1980-2014 average, there were many newsworthy storms which caused widespread damage
 262 and disruption across the UK including the aforementioned Xaver and Christian (the ‘St
 263 Jude’s Day’ windstorm 28th October 2013), the latter shown to have produced a SJ [*Browning*
 264 *et al.*, 2016].

265

266 Some ETCs are on a very small scale and contain exceptionally strong winds, e.g. Christian
 267 (8 top 1%DMGSs, 5 of which were 0.1%DMGSs), compared to events which stand out on a
 268 more national scale, such as storm Emma (29th February 2008; 25 1%DMGSs but no
 269 0.1%DMGSs). Two events which attracted much media coverage in Europe between 2008
 270 and 2014 were Windstorms Klaus (January 2009) and Xynthia (March 2010) but the track of
 271 these left the UK unscathed in terms of 1%DMGSs at any of the network sites.

272

273 3.3 2008-2014 climatology for sub-synoptic-scale feature contributions to 1%DMGS

274 Subjectively classified features associated with all DMGSs, from each of the 73 ETC events,
 275 are summarised in Table 2.

276

277 **Table 2.** 2008-2014 Sub-synoptic-scale features^a

| Gust causing mechanism | Total 1%DMGS (%) | Total 0.1%DMGS (%) | Percentage of 1%DMGSs also 0.1%DMGSs |
|--|-----------------------------|-----------------------------------|---|
| Returning cold conveyor belt (CCBb) | 205 (34.2%) | 9 (22%) | 4.4% |

| | | | |
|--|-------------|------------|-------|
| Warm conveyor belt (WCB) | 100 (16.7%) | 4 (9.8%) | 4% |
| Convective line (CL) | 78 (13%) | 10 (24.4%) | 12.8% |
| Pseudo-CL | 74 (12.3%) | 6 (14.7%) | 8.1% |
| Cold conveyor belt (CCBa) | 31 (5.2%) | 1 (2.4%) | 3.2% |
| Dry conveyor belt (DCB) | 30 (5%) | 1 (2.4%) | 3.3% |
| Convective systems (CS) and Dry slot convective systems (DSCS) | 23 (3.8%) | 0 | 0 |
| Potential Sting Jet (SJ) | 21 (3.5%) | 10 (24.4%) | 47.6% |
| Unclassified | 38 (6.3%) | 0 | 0 |
| Total | 600 | 41 | |

278 ^a2008-2014 Sub-synoptic-scale features associated with the top 1% and 0.1% of DMGSs.
279 Note - thresholds are based on the full 1980-2014 dataset, hence the proportion of 1%DMGS
280 to 0.1%DMGS is not 10%.

281

282 Over the 2008-2014 period, the CCBb accounted for over 34% of all 1%DMGS, the WCB
283 being the second most influential feature. These conveyor belts are widely known to regularly
284 cause extreme surface winds within ETCs [e.g. *Browning, 2004; Hewson and Neu, 2015*] and
285 the results are comparable, proportionally, to those of *Parton et al. [2010]* who focused on
286 the mid-troposphere. The CCBa only accounted for 5% of 1%DMGSs, highlighting that this
287 part of the CCB feature is far less likely to be associated with extreme winds than the CCBb.
288 1%DMGSs associated with CCBbs occurred over the whole UK apart from the southern
289 coast of England. 1%DMGSs associated with the WCB also occurred over all parts of the
290 country, which is unsurprising given the typically large area of the WCB relative to some of
291 the other identified features [*Hewson and Neu, 2015; Table 1*]. The CCB (a and b combined)

292 and WCB account for far fewer 0.1%DMGSs, showing that while causing wide-spread strong
293 winds, they are not so often associated with the most severely damaging (top 0.1%) winds.

294

295 Table 2 demonstrates the importance of CLs in the production of damaging winds in the UK.
296 *Clark* [2013] showed that CLs occur frequently in the UK during the autumn and winter
297 months and the results here indicate that they are also very influential in causing some of the
298 most extreme UK surface winds, accounting for over 13% of 2008-2014 1%DMGS and
299 almost a quarter of all 0.1%DMGSs. The spatial distribution of CLs (not shown) has them
300 mostly located in the southern half of the UK, in accordance with *Clark* [2013], CLs often
301 dissipating on encountering the mountainous topography of the interior of northern Britain.
302 An exception to this occurred however during windstorm *Xaver* where nine of the eleven
303 1%DMGSs in northern Britain were attributed to these features occurring as two organised
304 bands of heavy precipitation passing over the area, associated with primary and secondary
305 cold fronts. Six of these were 0.1%DMGSs, showing that these systems can cause highly
306 damaging winds anywhere in the UK.

307

308 Pseudo-CLs (Table 1) were associated with just over 12% of the 1%DMGS and 15% of
309 0.1%DMGSs, including fronts, troughs and pre-/post-CL (not shown) situations during
310 windstorms. These occurred during the 'cool season' (September-February) and were not
311 large enough spatially, long enough temporally or intense enough to feature in *Clark's* [2013]
312 CL climatology. However they still produced extreme surface wind speeds, indicating that
313 the *Clark* [2013] CL threshold criteria (Table S1), designed primarily to identify the more
314 extensive and intense examples of narrow cold-frontal rain bands, may be too rigid for
315 directly re-purposing to UK extreme wind gust applications. The latter is further supported by
316 the geographical distribution of pseudo-CLs here being less weighted towards the south of
317 the UK, implying that 2008-2014 CLs in the north were generally less strong, less long-lived
318 and less extensive. However, CL frequencies in *Clark's* [2013] 2003-2010 climatology were
319 non-zero over most of the north of the UK, so CLs are not completely unknown in this region
320 as exemplified by windstorm *Xaver*. CLs and Pseudo-CLs (when combined) are very
321 important contributors to UK extreme winds, accounting for over a quarter of 1%DMGSs and

322 more than a third of 0.1%DMGSs, making them the most important ETC mechanism for
323 producing extreme surface winds.

324

325 During the 2008-2014 period, there were at least three known SJ producing ETC in the
326 literature, Friedhelm on 8th December 2011 [*Baker et al., 2013; Martinez-Alvarado et al.,*
327 2014, *Vaughn et al., 2015*], Ulli on 3rd January 2012 [see *Smart and Browning, 2014*] and
328 Christian on 28th October 2013 [*Browning et al., 2016*]. SJs were also allocated as the cause
329 of 0.1%DMGSs during each of these events during our study. 21 of the 600 1%DMGS were
330 diagnosed as potentially being caused by SJs. Over 10 ETCs were originally considered as
331 potentially including SJs based on the location of the gust, and cloud head, but were
332 subsequently shown to have an insufficient central pressure deepening rate [*Browning, 2004*]
333 and/or there was no obvious evidence of cloud banding in satellite images (not shown). So
334 the closely located CCBb is the feature most likely associated with these gusts. It has not
335 been possible here to effectively distinguish between SJs and the CCBb during frontal ‘T-
336 bone’ development (stage III and between III-IV) using the observational and relatively
337 coarse model output tools available (ERA-interim), hence these 21 1%DMGS remain
338 ‘potential’ SJs [see *Martinez-Alvarado et al., 2014*]. These events are an important set. Of the
339 21 1%DMGSs, 10 (47.6%) are also 0.1%DMGSs, showing how extreme they can be, making
340 up almost a quarter of all 0.1%DMGSs. This continues the pattern, along with CLs, of
341 smaller scale features producing the most damaging (top 0.1%) gusts.

342

343 A northern and western UK spatial distribution of potential SJs is seen in our study, with the
344 exception of windstorm Christian which produced potential SJs over the south of England at
345 seven different sites (Figure S2). A possible reason for this is that SJs occur mid-way through
346 an ETC’s life cycle, during or just after the rapid deepening of ETCs that form in the genesis
347 region in the relatively warm waters of the eastern Atlantic; ETCs are more likely to form and
348 develop over the sea than over land [*Dacre and Gray, 2009*]. This implies less rapid
349 deepening and therefore less SJ potential over eastern UK locations, eastward tracking ETCs
350 losing their energy source once they reach land. However, when they do reach this region,
351 they have a major impact. *Browning [2004]* found that for the October 1987 storm, a SJ
352 formed in eastern England, though the exceptional SW-NE orientation of this track may have

353 added to the low-level convectonal forcing of this ETC from the relatively warm English
354 Channel. This meant that the ETC was still intensifying when it reached the south coast of
355 England, unlike the majority of east Atlantic forming storms that have a more W-E track
356 [Dacre and Gray, 2009]. This is similar to the track observed during windstorm Christian.
357 We are not aware of a previous study of the geographical spread of surface SJs as we
358 highlight in Figure S2; *Martínez-Alvarado et al.* [2012] did highlight the SJ precursor areas in
359 relation to the ETC centre, indicating that tracks of such cyclones tended to begin further
360 south than the general average. All other SJ-related publications are case study based.
361 *Hewson and Neu*, [2015] indicate the position of SJs in relation to the storm track, though this
362 is not based on surface observations.

363

364 The 0.1%DMGS results highlight the importance of some sub-synoptic-scale features which
365 are perhaps not always given the attention that their surface impacts merit. There is currently
366 much concentration in the literature on the formation of SJs responsible for extreme gusts
367 within ETCs [Browning, 2004; Clark et al., 2005; *Martínez-Alvarado et al.*, 2012; *Smart and*
368 *Browning*, 2013; *Browning et al.*, 2016]. Our results suggest that greater focus could also be
369 usefully paid to CL/pseudo-CL features which, based on the station network utilised here, are
370 associated with a third of the most damaging observed UK surface gusts during the 2008-14
371 period.

372

373 **4. Conclusions**

374 The main objective of this paper was to construct a 2008-2014 climatology of UK ETC sub-
375 synoptic-scale features associated with the highest surface wind gusts recorded across a
376 network of UK surface stations. A novel way to quantify the relative contributions of
377 mesoscale ETC features was introduced. We demonstrate that larger scale features (WCB and
378 CCB) dominate the top 1% of UK extreme winds, however it is the smaller scale
379 mechanisms, CLs and SJs, which produce the most intense (top 0.1%) gusts. The CCB, is
380 split into two categories, ahead of the warm front (CCBa) and when returning from the
381 poleward side of the low pressure centre (CCBb)). The CCB is most hazardous when joining
382 the direction of ETC travel, during CCBb, accounting for 34% of 1%DMGSs and 22% of

383 0.1%DMGSs, whereas the CCBa accounts for 5% and 2% respectively. CLs and pseudo-CLs,
384 account for 13% and 12% respectively of the top 1% of DMGSs, and also greatly influence
385 the top 0.1% (24% and 15% respectively); convective lines merit more attention. Potential
386 SJs account for 3.5% of 1%DMGSs but these events are particularly significant, almost half
387 also being categorised as 0.1%DMGSs, accounting for 24% of the strongest winds seen at
388 UK observation stations in this period despite their small scale nature.

389

390 Going forward, we plan to extend this 2008-2014 climatology into the future. A recent study
391 by Schemm et al. (2016), has indicated that extremely active fronts are becoming more
392 frequent over Europe, especially since the year 2000, so this work will become crucial in our
393 understanding of the UK wind regime in a changing climate. We also plan conduct seasonal
394 analysis on the individual ETC features identified in this study.

395

396 **Acknowledgements**

397 This research was kindly funded by the Worshipful Company of Insurers and the Australian
398 Research Council Grant DP16010997. Our thanks go to the UK Met Office for providing the
399 windspeed and radar data via the British Atmospheric Data Centre (BADC; available at
400 http://badc.nerc.ac.uk/data/ukmo-midas/ukmo_guide.html). We would also like to
401 acknowledge the University of Dundee Satellite Receiving Station (available at
402 <http://www.sat.dundee.ac.uk/>) for access to satellite imagery and Richard Hewston for his
403 part in the creation of the DMGS database. Our thanks goes to Matthew Clark, who provided
404 useful feedback on the ‘convective lines’ part of the project. We would also like to
405 acknowledge the contribution of the late Roland von Glasow, who was highly influential in
406 the early discussions of this work, providing exceptional insight and knowledge.

407

408

409

410

411

412

413

414

415

416 **References**

417 Baker, L (2009), Sting jets in severe northern European wind storms, *Weather*, 64 **6**, 143-148.

418 Baker, L., O. Martinez-Alvarado, J. Methven, and P. Knippertz (2013), Flying through
419 extratropical cyclone Friedhelm, *Weather*, 68 **1**, 9-13.

420 Bjerknes, J., and H. Solberg (1922), *Life cycle of cyclones and the polar front theory of*
421 *atmospheric circulation*, pp18. Grondahl.

422 Brönnimann, S., O. Martius, H. von Waldow, C. Welker, J. Luterbacher, G. P. Compo, P. D
423 Sardeshmukh and T. Usbeck (2012), Extreme winds at northern mid-latitudes since
424 1871, *Meteorologische Zeitschrift*, **21**(1), 13-27.

425 Browning, K. A. (1990), Organization of clouds and precipitation in extratropical cyclones.
426 Extratropical Cyclones: The Erik Palmén Memorial Volume, C. W. Newton and E. O.
427 Holopainen, Eds, *Amer. Meteor. Soc.*, 129-153.

428 Browning, K. A (2004), The sting at the end of the tail: Damaging winds associated with
429 extratropical cyclones, *Q. J. Roy. Meteor. Soc.*, **130**(597), 375-399.

430 Browning, K. A., D. J. Smart, M. R. Clark, and A. J. Illingworth (2015), The role of
431 evaporating showers in the transfer of sting-jet momentum to the surface, *Q. J. Roy. Meteor.*
432 *Soc.*, **141**(693), 2956-2971.

433 Carlson, T. N. (1980), Airflow Through Midlatitude Cyclones and the Comma Cloud Pattern,
434 *Mon. Wea. Rev.*, **108**, 1498–1509.

435 Clark, M. R. (2013), A Provisional Climatology of Cool-Season Convective Lines in the UK,
436 *Atmos. Res.*, **123**,180-196.

437 Clark, P. A., K. A. Browning, and C. Wang (2005), The sting at the end of the tail: Model
438 diagnostics of fine-scale three-dimensional structure of the cloud head, *Q. J. Roy. Meteor.*
439 *Soc.*, **131**(610), 2263-2292.

440 Cotton, W. R., and R. A. Anthes (1989), *Storm and Cloud Dynamics*, Int. Geophys. Series,
441 Vol. 44, 883pp. Academic Press.

- 442 Dacre, H. F., and S. L. Gray (2009), The Spatial Distribution and Evolution Characteristics of
443 North Atlantic Cyclones, *Mon. Weather. Rev.*, **137**, 99-115.
- 444 Dacre, H. F., M. K. Hawcroft, M. A. Stringer, K. I. Hodges (2012), An Extratropical Cyclone
445 Atlas: A Tool for Illustrating Cyclone Structure and Evolution Characteristics, *Bull. Am.*
446 *Meteorol. Soc.*, **93**(10), 1497-1502.
- 447 Davis, C., et al. (2004), The Bow Echo and MCV Experiment, *Bull. Amer. Meteor. Soc.*, **85**,
448 1075-1093.
- 449 Earl, N. (2013), The UK wind regime-Observational trends and extreme event analysis and
450 modelling, PhD Thesis, *University of East Anglia*.
- 451 Earl, N., S. Dorling, R. Hewston, and R. von Glasow (2013), 1980-2010 variability in UK
452 surface wind climate, *J. Clim.* **26**, 1172–1191. doi:10.1175/JCLI-D-12-00026.1.
- 453 Gatzen, C., T. Púčik, and D. Ryva (2011), Two cold-season derechos in Europe, *Atmos.*
454 *Res.*, **100**(4), 740-748.
- 455 Gray, S. L., O. Martínez-Alvarado, L. H. Baker, and P. A. Clark (2011), Conditional
456 symmetric instability in sting-jet storms, *Q. J. R. Meteor. Soc.*, **137**(659), 1482-1500.
- 457 Hanna, E., T. E. Cropper, P. D. Jones, A. A. Scaife, and R. Allan (2015), Recent seasonal
458 asymmetric changes in the NAO (a marked summer decline and increased winter variability)
459 and associated changes in the AO and Greenland Blocking Index, *Int. J. Clim.*, **35**(9), 2540-
460 2554.
- 461 Hewson, T. D., and U. Neu (2015), Cyclones, windstorms and the IMILAST project, *Tellus*
462 *A*, **67**, 27128.
- 463 Hewston, R (2008), Weather, Climate and the Insurance Sector, PhD Thesis, *University of*
464 *East Anglia*.
- 465 Hewston, R., and S. R. Dorling (2011), An analysis of observed maximum wind gusts in the
466 UK, *J. Wind. Eng. Ind. Aerod.* **99**, 845-856. doi:10.1016/j.jweia.2011.06.004
- 467 Lamb H.H (1950) Types and spells of weather around the year in the British Isles: Annual
468 trends, seasonal structure of the year, singularities. *Quart. J. Royal Met. Soc.* **76**/330, pp393-
469 438.
- 470 Martínez-Alvarado, O., S. L. Gray, J. L. Catto and P. A. Clark (2012), Sting jets in intense
471 winter North-Atlantic windstorms, *Environ. Res. Lett.* **7** 024014
- 472 Martínez-Alvarado, O., L. H. Baker, S. L. Gray, J. Methven, and R. S. Plant (2014),
473 Distinguishing the cold conveyor belt and sting jet airstreams in an intense extratropical
474 cyclone, *Mon. Wea. Rev.*, **142**(8), 2571-2595.
- 475 Neu, U., et al. (2013). IMILAST: a community effort to intercompare extratropical cyclone
476 detection and tracking algorithms, *Bull. Amer. Meteor. Soc.*, **94**(4), 529-547.

- 477 Parton, G. A., G. Vaughan, E. G. Norton, K. A. Browning, and P. A. Clark (2009), Wind
478 profiler observations of a sting jet, *Q. J. R. Meteor. Soc.*, **135**(640), 663-680.
- 479 Parton, G. A., A. Dore, and G. Vaughan (2010), A climatology of midtropospheric mesoscale
480 strong wind events as observed by the MST radar, Aberystwyth, *Meteor. Appl.*, **17**, 340–354,
481 doi:10.1002/met.203.
- 482 Schemm, S., M. Sprenger, O. Martius, H. Wernli, and M. Zimmer (2016), Increase in the
483 number of extremely strong fronts over Europe?—A study based on ERA-Interim reanalysis
484 (1979–2014), *Geophys. Res. Lett.* In print, doi: 10.1002/2016GL071451
- 485 Schultz, D. M., D. Keyser, and L. F. Bosart (1998), The effect of largescale flow on low-level
486 frontal structure and evolution in midlatitude cyclones, *Mon. Wea. Rev.*, **126**, 1767–1791.
- 487 Schultz, D. M., and G. Vaughan (2011), Occluded fronts and the occlusion process: A fresh
488 look at conventional wisdom, *Bull. Am. Meteorol. Soc.*, **92**, 443–466 ES19–ES20.
- 489 Schultz, D. M. (2001), Reexamining the cold conveyor belt, *Mon. Wea. Rev.*, **129**, 2205-2225.
- 490 Shapiro, M. A., and D. Keyser (1990), Fronts, jet streams and the tropopause. Extratropical
491 Cyclones, The Erik Palmén Memorial Volume, C. W. Newton and E. O. Holopainen, Eds.,
492 *Amer. Meteor. Soc.*, 167–191.
- 493 Smart, D. J., and K. A. Browning (2014), Attribution of strong winds to a cold conveyor belt
494 and sting jet, *Q. J. R. Meteorol. Soc.*, **140**(679), 595-610.
- 495 Swiss Re. (2016), Natural Catastrophes and man-made disasters in 2015: historic losses
496 surface from record earthquakes and floods, *Sigma*, No 1/2016
- 497 Tilinina, N., S. K. Gulev, I. Rudeva, and P. Koltermann (2013), Comparing cyclone life cycle
498 characteristics and their interannual variability in different reanalyses, *J. Clim.*, **26**(17), 6419-
499 6438.
- 500 Vaughan, G., et al. (2015), Cloud banding and winds in intense European cyclones: Results
501 from the DIAMET project, *Bulletin of the American Meteorological Society*, **96**(2), 249-265.
- 502 Vautard, R., J. Cattiaux, P. Yiou, J. Thépaut, and P. Ciais (2010), Northern Hemisphere
503 atmospheric stilling partly attributed to an increase in surface roughness, *Nat. Geosci.* **3**, 756-
504 761. doi: 10.1038/NGE0979
- 505 Wang, X. I., F. W. Zwiers, V. R. Swail, and Y. Feng (2009), Trends and variability of
506 storminess in the Northeast Atlantic region, 1874-2007. *Clim. Dynam.* **33**, 1179-1195.
- 507 Weisman, M. L. (2001), Bow echoes: A tribute to TT Fujita, *Bull. Am. Meteorol. Soc.*, **82**(1),
508 97-116.
- 509 Wheatley, D. M., R. J. Trapp, and N. T. Atkins (2006), Radar and damage analysis of severe
510 bow echoes observed during BAMEX, *Mon. Weather Rev.*, **134**(3), 791-806.

511 Woodroffe, A. (1988), Summary of weather pattern developments of the storm of 15/16
512 October 1987, *Meteor. Mag.*, **117**, 99–103.

513

514